International Research Journal of Innovations in Engineering and Technology (IRJIET)

ISSN (online): 2581-3048
Volume 6, Issue 6, pp 118-125, June-2022
https://doi.org/10.47001/IRJIET/2022.606015

Three-Dimensional CFD Simulations of Transient Cavitation in a Centrifugal Pump

[1]*Hani M. S. Salman, [2]Amir S. Dawood, [3]Younis M. Najim

[1]Department of Electronic Engineering, College of Electronics Engineering, Ninevah University, 42002, Iraq
[2,3]Department of Mechanical Engineering, College of Engineering, University of Mosul, 42002, Iraq
*Corresponding Author: hani.enp160@student.uomosul.edu.iq

***Abstract* - Liquid pumps can be found in many industrial and domestic applications. In several operating circumstances where the inlet pressure and pump flow varies to a point where the pump performance crashes due to cavitation. On long term effect, the cavitation can cause material loss to the impeller blade and eventually damages the pump impeller. This study present meanline analysis to construct pump impeller and volute. The three-dimensional pump impeller model is then generated using Bezier polynomial that fits the inlet and outlet main geometrical parameters obtained from the meanline and create the hub, shroud and blade profiles. The meanline design is also used to determine the design flow and operating. Three-dimensional, CFD analysis is then conducted to study the evolution of the cavitation in the impeller of the centrifugal pump under variable inlet pressure. The inlet total pressure is allowed to decrease with time from atmospheric value to a point where the cavitation is fully developed in the pump impeller until the pump head is dropped near zero. The Rayleigh-Plesset homogenous cavitation model coupled with incompressible Navier-Stokes solver successfully reproduces the blade suction and pressure sides, pressure recovery in the volute extension, homogenous distribution of the pressure across the interface between moving impeller and fixed volute. The CFD results uncover three distinct phases of the cavitation evolution in the pump undergoing transient drop in the inlet pressure; phase (1) remarks the start of the cavitation where no impact is seen on the developed head, phase (2) indicates the rapid grow and propagation of the cavitation along the suction side from leading to trailing edge of the impeller blade, and finally phase (3) where the cavitation blocks the space between the blades and pump head drops down to zero. A generalized behavior is seen for the flow structure as the flow is streamed in phases one. Vortical (circulation) flow is developed in phase two and back to streamed flow during phase three by virtue of displacing more flow due to dramatic increase in the specific volume.**

Keywords: CFD, Cavitation, Centrifugal pump performance.

I. INTRODUCTION

The flow in a centrifugal pump is characterized by three-dimensional variations, high turbulent intensity, and multiple frames of references (MFR). The computational fluid dynamics has significantly contributed to reproducing the flow structure and predicting a centrifugal pumps performance. The experimental analysis has verified the capabilities of the CFD tools. However, CFD analysis requires realistic boundary and initial conditions which are commonly determined by using either experimental measurement or meanline one-dimensional analysis. The cavitation flow in a centrifugal pump is, however, remains imposing a challenge in computational fluid dynamics since the phenomena are characterized by two-phase, turbulent flow. The interface between liquid and vapor is main obstacle that requires reliable numerical schemes to be tracked accurately. The study of flow in a centrifugal pump under cavitation environments has gained more momentum in recent years following the advancement of computational and algorithms development. Furthermore, cavitation is known as an inconvenient class of flow that significantly reduces the performance of a pump and erosion (or pitting) of the impeller material.

The effect of blades number and outlet pressure on pump performance characteristics were investigated by Alex George and Dr. P Muthu [1]. The cavitation evolution for different blade number and outlet pressure was also included. It was found that the optimal blade number for best efficiency and cavitation characteristics is 7 and 5. The needed head is rather high for a pump with seven impeller blades. The optimum outlet pressure for the minimum vapor fraction (or cavitation) was about 305000 Pa. Furthermore, the CFD tool was also used by Wilson Sánchez Ocaña et al [2]to develop and analyze the cavitation phenomena in the impeller of the centrifugal pump. A choking technique was used to investigate the cavitation phenomenon in the eye of the pumping impeller in which the ball valve located in the suction pipe was closed at an angle of 45° to reduce the inlet pressure. The inlet pressure was decreased experimentally from 42.75 kPa to 19.31 kPa. The findings demonstrated how the fluid behaves as it

International Research Journal of Innovations in Engineering and Technology (IRJIET)
ISSN (online): 2581-3048
Volume 6, Issue 6, pp 118-125, June-2022
https://doi.org/10.47001/IRJIET/2022.606015

transitions from a liquid to a steam condition, resulting in the development of vapor bubbles whose implosion causes the impeller surface to wear down. The regions influenced by cavitation were estimated. To achieve optimal performance of a certain centrifugal pump, the blade angle distribution along leading edge were investigated by Y Xu et al [3] using computational fluid dynamics (CFD). Three distinct sets of blade angle distributions along the leading edge were selected for three various blade intake angles in order to create nine centrifugal pumps with different impellers and same volute. The cavitation model wasZwart-Gerber-Belamriwhich is based on the Rayleigh-Plesset equation. The numerical findings are verified with experimental data and demonstrated that the numerical simulation can properly predict centrifugal pump cavitation performance. The better distribution method was the equally distributed method, and the most efficient average value of the inlet blade angle is 49°. The other methods are nearly identical in their performance. The cavitation began initially on the leading edge of the suction side at the impeller hub and subsequently propagated across the whole passageway. Also, the region of cavitation increased from the hub to the shroud while the value of NPSHa decreased. The shape of the intake has a significant impact on the cavitation performance of the system. It was found that the cavitation in pumps can be reduced by maintain uniform flow rate through selecting appropriate inlet parameters. Furthermore, the cavitation Rayleigh-Plesset model which based on bubble growth and implosion was also used by S F Xieet al[4]to enhance the cavitation performance of the centrifugal pump by having slots on the impeller blade near the entrance. Six distinct hydraulic model groups were generated for this purpose. The results indicated that the cavitation performance can be improved by slots on blade near inlet. Under the same operating flow conditions, the pressure on the blade suction side near inlet was higher in the slotted blade than the unmodified blade and the head developed experienced small change while the flow energy distribution between the two blades was more uniform.

This work presents a CFD study of cavitation evolution in a centrifugal pump impeller and volute under transient drop in inlet total pressure. The pump impeller is design using meanline analysis. The Rayleigh Plesset Model is used to model the cavitation phenomena.

II. MODELING

Two main schemes used to model the centrifugal pump. The first one is the meanline scheme which is used to generate the main geometrical parameters (see Figure (1)) and flow conditions at the inlet and outlet of the pump. The meanline scheme is based on one-dimensional analysis and uses fundamental physics such as continuity and momentum equations. Since this analysis is simple and unable to accurately predict the viscus and circulation losses, empirical correlations are incorporated into the analysis to enhance the accuracy of the pump performance. The meanline analysis is conducted using in-house MATLAB code. The input design parameters of the meanline scheme are presented inTable (1):

Table (1): Required operating conditions

Descriptions	value	Unit
Flow Rate [Q]	60	m^3/h
rotational Speed [n]	2900	rpm
Required Head [H]	39	m
Operating Temperature [T]	25	℃
Water Density [ρ] at 25 ℃	997	kg/m^3
Suction Pressure [P_1]	1	bar
Discharge Pressure [P_2]	4.819	bar
Viscosity of Water [μ] at 25 ℃	0.0008899	$k / m \cdot s$

Since the meanline analysis is unable to reproduce the cavitation phenomenon, three-dimensional, CFD analysis is then introduce to investigate the effect of cavitation on the pump performance and flow structure. To generate the three-dimensional computational domain, Bezier polynomial is then used to connect the inlet and outlet geometrical parameters and generate the three-dimensional profiles of the impeller's blade, hub and shroud. The thee-dimensional model is then discretized using state of art mesh generation tool known as TurboGrid which generates hexahedral computational cells and enables CFD solver to use high order numerical schemes. The mesh is tested and versified using mesh independent test to ensure that the mesh size is capable of reproducing the variation of flow variables everywhere in the flow domain. The meanline output parameters are listed inTable (2).

Table (2): The geometrical parameters of the impeller and volute

Impeller geometrical output parameters	
Number of main blades	6
Impeller inlet diameter	77.7 mm
Impeller exit diameter	181.6 mm
Blade angle of the impeller trailing edge (backward)	37.1°
Blade angle of the impeller leading edge	18.9°

International Research Journal of Innovations in Engineering and Technology (IRJIET)

ISSN (online): 2581-3048

Volume 6, Issue 6, pp 118-125, June-2022

https://doi.org/10.47001/IRJIET/2022.606015

The angle between streamlines and shaft at the impeller inlet	0°
The angle between streamlines and shaft at impeller exit	90°
The axial length of the impeller	41 mm
Impeller passage width at the inlet	22.1 mm
Impeller passage width at the outlet	10.6 mm
Blade thickness at impeller leading edge	2.6 mm
Blade thickness at impeller trailing edge	3 mm
Volute geometrical output parameters	
Volute Base Circle	199.8 mm
Volute Inlet Width	21.1 mm
Volute throat Area	1441.4 mm^2

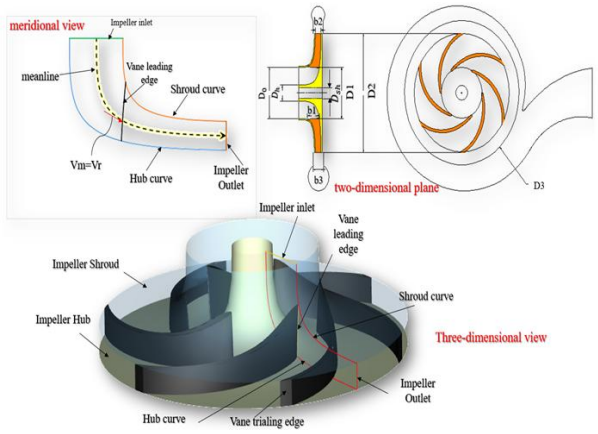

Figure (1): Pump's three-dimensional view and two-dimensional plane, with representation of meridional plane

The three-dimensional Reynolds Averaged Navier Stokes (RANS) are solved in the CFD analysis using available CFX solver from ANSYS[5].The shear stress transport turbulence model (also known as Menter's Model) is used to address the closure problem of RANS. The RANS equations are based on assumptions that the flow is incompressible, turbulent, viscus, three-dimensional, and in unsteady state condition.

Since the flow is incompressible, the governing equations consist of the continuity and momentum equations only as:

Continuity:

$$\nabla \bar{U} = 0 \quad \text{Eq(1)}$$

Momentum:

$$\frac{\partial(\bar{\mathbf{U}})}{\partial t} + \nabla \cdot (\bar{\mathbf{U}} \otimes \bar{\mathbf{U}}) = -\frac{1}{\rho}\nabla \bar{P} + \nabla \cdot \nu_{\text{eff}} \left[\nabla \bar{\mathbf{U}} + (\nabla \bar{\mathbf{U}})^T - \frac{2}{3}\delta \nabla \cdot \bar{\mathbf{U}}\right] + \frac{1}{\rho} S_{\text{rot}} + \frac{1}{\rho} S_{\text{cav}} \quad \text{Eq(2)}$$

It can be noted that there is no need to incorporate the transient term in the continuity equation since the fluid density remains unchanged. ∇ is a differential, directional, methematical operaor sujected here on the fluid peroperty. $\bar{\mathbf{U}}$ is the mean flow velocity vector in the three- dimensional space. $\bar{P}$ is the mean fluid pressure. ν_{eff} is the effective viscosity that is the sum of molecular kinematic viscosity and eddy (turbulent) viscosity. S_{rot} is used to account for Coriolis and centrifugal forces as they developed in the fluid flow in a rotating frame of reference such as:

$$S_{\text{rot}} = -2\omega \times \bar{\mathbf{U}} - \omega \times (\omega \times \mathbf{r}) \quad \text{Eq(3)}$$

Where ω is a constant impeller angular velocity vector with one component is since the impeller rotates about one-axis only.

Modeling of Cavitation Source Term:

In the incompressible liquid flow, when the pressure is dropped below the saturated vapor pressure, the liquid is vaporized, and its volume increases by almost three orders of magnitude. This process can occur locally in certain regions of the centrifugal pump impeller, and it is sometime known as a hydraulic cavitation in contrast to the thermal phase change. The cavitation model is activated by a parameter known as cavitation number which is designed to track the local pressure at every computational cell. The cavitation number is defined as:

$$\frac{dV_b}{dt} = \frac{d}{dt}\left(\frac{4}{3}\pi R_b^3\right) = 4\pi R_b^2 \left[\sqrt{\frac{2}{3}\frac{P_v - P}{\rho}}\right] \quad \text{Eq(4)}$$

$$C_a = \frac{p - P_v}{\frac{1}{2}\rho \bar{U}^2} \quad \text{Eq(5)}$$

It should be noted that P denoted to the reference local liquid pressure which is taken as the liquid pressure surround the region in which the cavitation is developing. P_v is the vapor saturation pressure determined at the liquid temperature. The denominator represents the dynamic pressure at each cell. The time scale of the hydraulic cavitation is fast and thermodynamic equilibrium at the interface between fluid liquid and vapor is well accepted. The cavitation is modeled simply by introducing the amount of mass transfer from the liquid to vapor which is derived the liquid-vapor pressure difference rather than thermal effect.

International Research Journal of Innovations in Engineering and Technology (IRJIET)

ISSN (online): 2581-3048

Volume 6, Issue 6, pp 118-125, June-2022

https://doi.org/10.47001/IRJIET/2022.606015

In this research, the Rayleigh Plesset Model is implemented to model the cavitation in a centrifugal pump undergoing transient decrease in the inlet pressure. This model is based on rate of gas bubble growth/or shrink in a homogeneous mixture and the rate of change of gas bubble change can be expressed as[6];

$$R_b \frac{d^2R_b}{dt^2} + \frac{3}{2}\left(\frac{dR_b}{dt}\right)^2 + \frac{2\sigma}{\rho R_b} = \frac{P_v - P}{\rho} \qquad \text{Eq (6)}$$

Here R_b is the bubble radius and σ represent the surface tension coefficient between the liquid and vapor. The equation above derived from mechanical balance and no thermal balance is incorporated as our case assumes the density and hence the temperature remains unchanged.

Since no high frequencies oscillation is developed in the flow, the second order derivative term is neglected, and the equation becomes:

$$\frac{dR_b}{dt} = \sqrt{\frac{2}{3}\frac{P_v - P}{\rho}} \qquad \text{Eq (7)}$$

The rate of change of bubble volume is expressed as:

The fluid density is assumed constant and the rate of change of bubble mass can be derived by multiplying the volume rate of change by fluid vapor density:

$$\frac{dm_b}{dt} = 4\pi\rho_g R_b^2 \left[\sqrt{\frac{2}{3}\frac{P_v - P}{\rho}}\right] \qquad \text{Eq (8)}$$

Let's introduce number of bubbles per unit volume ($\zeta = V_b N_b$) as the volume of one bubble times number of bubbles. The total mass transfer that crosses the inter phase per unit volume is then defined as:

$$\dot{m}_{fg} = N_b \frac{dm_b}{dt} = \frac{\zeta}{V_b}\frac{dm_b}{dt} = \frac{3\zeta\rho_g}{R_b}\left[\sqrt{\frac{2}{3}\frac{P_v - P}{\rho}}\right] \qquad \text{Eq (9)}$$

To incorporate the condensation effect, this equation is modified as:

$$\dot{m}_{fg} = \frac{3\zeta\rho_g}{R_b}\left[\sqrt{\frac{2}{3}\frac{P_v - P}{\rho}}\right][\Psi \text{ sign } (P - P_v)] \qquad \text{Eq (10)}$$

The literature studies have shown that vaporization is started at nucleation regions where the liquid is about to change the molecular structure and undergo phase change. As the volume fraction of vapor increases, the nucleation regions density must decrease accordingly due to less liquid remains in hand. Therefore, the total mass transfer that crosses the inter phase per unit volume is then modified as:

$$\dot{m}_{fg} = \frac{3(1-\zeta)\rho_g\zeta_{nuc}}{R_{nuc}}\left[\sqrt{\frac{2}{3}\frac{P_v - P}{\rho}}\right][\Psi \text{ sign } (P_v - P)] \qquad \text{Eq (11)}$$

Here ζ_{nuc} is the vapor volume fraction of the nucleation spots. In this work, $R_{nuc} = 0.001$ mm, $\zeta_{nuc} = 5 \times 10^{-4}$, $\Psi = 50$ for evaporation and 0.01 for condensation as suggested by [7].

Boundary Conditions:

One of the main reasons of starting with meanline, one-dimensional analysis is to estimate the flow conditions at the inlet and outlet of the centrifugal pump under prespecified operating conditions. Since the flow is assumed incompressible and isothermal, the total pressure at the inlet is imposed. The meanline is used to determine the outlet mass flow rate. However, the way inlet total pressure is imposed at the inlet is a key parameter in this study and is decreased with time as shown in **Error! Reference source not found.**).

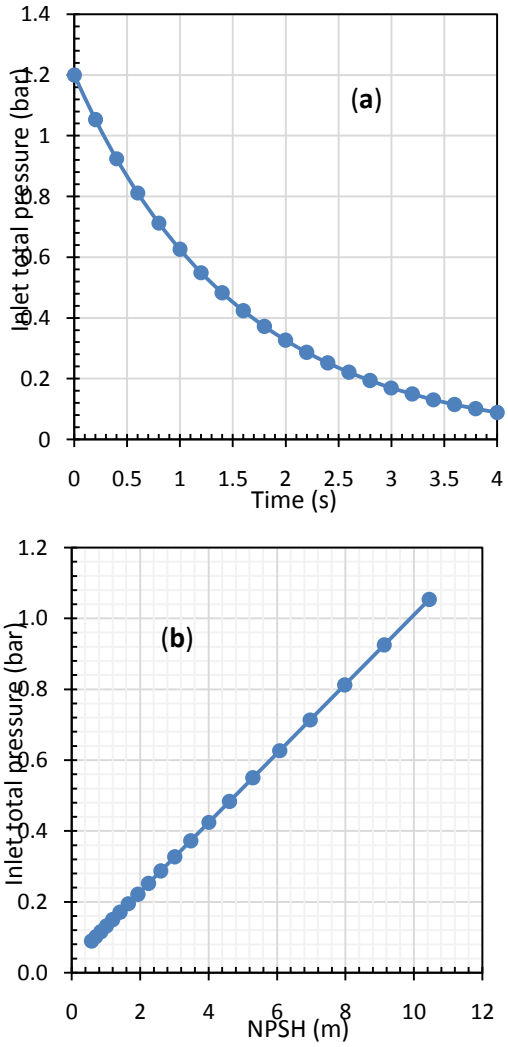

Figure (2): Inlet total pressure changes with respect to (a) Time, (b) NPSH

International Research Journal of Innovations in Engineering and Technology (IRJIET)

ISSN (online): 2581-3048

Volume 6, Issue 6, pp 118-125, June-2022

https://doi.org/10.47001/IRJIET/2022.606015

Mesh Generation:

The computational domain consists of three blocks: inlet blocks, impeller block and volute. Since the flow around each impeller blade is most likely statically similar, a periodic section of one impeller blade is only considered reducing the computational time while the volute is excluded from periodic section. The inlet and impeller sections are discretized using TurboGrid tool. This tool generates hexahedral computational elements with refined boundary layer region to ensure that the variation of the physical properties is accurately captured.

The volute domain is discretized using tetrahedral elements with refined mesh near walls regions to capture the large changes in flow velocity because of the viscosity and no-slip boundary conditions. Since the flow in both pump impeller and volute exhibit a nonlinear variation, it is difficult to assign averaged Reynolds number and determine the local hydraulic boundary layer thickness. To address this issue, the wall function model is set to auto-select option where the boundary layer regions with enough mesh resolution will be treated without wall function and the velocity gradient is captured on the grids. The wall function is activated only at the boundary layer region at which the mesh resolution is not enough. The non-dimensional distance Y-Pluse is used as a criterion for activating the wall function.

III. RESULTS AND DISCUSSION

Pump Performance without Cavitation:

In this section, we compile a parametric CFD study to investigate the performance of the designed centrifugal pump. This is essential step to make sure that the pump develops the design pressure head under prespecified operating conditions. The results can be viewed as a validation for the CFD analysis since the literature provides strong information on how pump head vary with the flow rate at the operating speed. (See Figure (3)) depicts the centrifugal pump efficiency and pressure head developed under different flow rate.

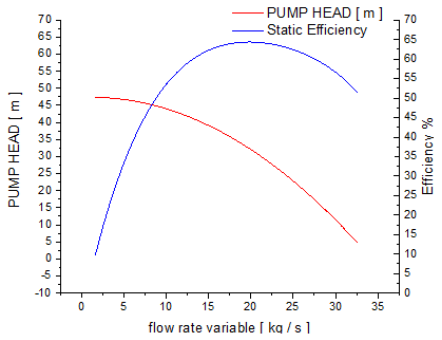

Figure (3): Characteristic performance curve of the designed pump

The pump head reaches maximum at about5kg/s followed by rapid decrease with nearly constant rate. On the other hand, the pump efficiency increases with flow rate and approaches maximum at about 20 kg/s and then exhibit a nonlinear and slow decrease with the flow rate. Similar behavior was reported by Li. et. al. [8].where the pump runsat speed of 2900 rpm, the impeller outlet diameter was 18.16 cm, and the design flow rate was 60 m3/h.

Pump Performance with Cavitation:

The flow structure, pressure field and evolution of cavitation in the pump impeller and volute at operating flow rate and speed are presented in this section. The velocity vector shown in Figure (4) demonstrates the effect of reducing total pressure at the pump inlet on the flow structure and velocity. When the inlet pressure at normal value (see Figure (4-a)), the flow is streamed in between the impeller blades as well as within the volute and no major vortical flow is observed. This concludes that the meanline is able to predict the blade profile under the design flow conditions. When inlet pressure is reduced to about 0.194 bar (seeFigure (4-b)),a flow circulation is developed in the suction side of the impeller blades which can be attributed to the increase of mean flow specific volume due to cavitation. Increasing the flow specific volume in a constant volume domain displaces more flow out of the domain and hence accelerates the flow velocity. However, it should be stressed that the flow velocity in this case is accelerating locally due to partial formation of water vapor leading to vortical flow. The cavitation is formed due to local decrease in the water static pressure. More importantly, the developed pump head remains unchanged because the amount of water being evaporated due to the cavitation is condensed back to liquid state downstream which recovers the head at the outlet (see Figure (4-c)).

When inlet pressure decreases further to 0.132 bar (see Figure (4-d)), the vapor volume fraction due to cavitation is dominant over liquid volume fraction, and the flow velocity is highly accelerated almost everywhere in the pump impeller due to the dramatic decrease in the fluid specific volume. At this condition, the flow back to streamed condition and no vortical flow is developed mainly due to effect of the cavitation which displaces more and more flow out of the impeller. Thus, no vortical flow is needed to fill the space. This must not be taken as a healthy indication, but it means that flow is accelerating even faster than the blade speed itself which result in a significant drop in the pump head.

International Research Journal of Innovations in Engineering and Technology (IRJIET)

ISSN (online): 2581-3048

Volume 6, Issue 6, pp 118-125, June-2022

https://doi.org/10.47001/IRJIET/2022.606015

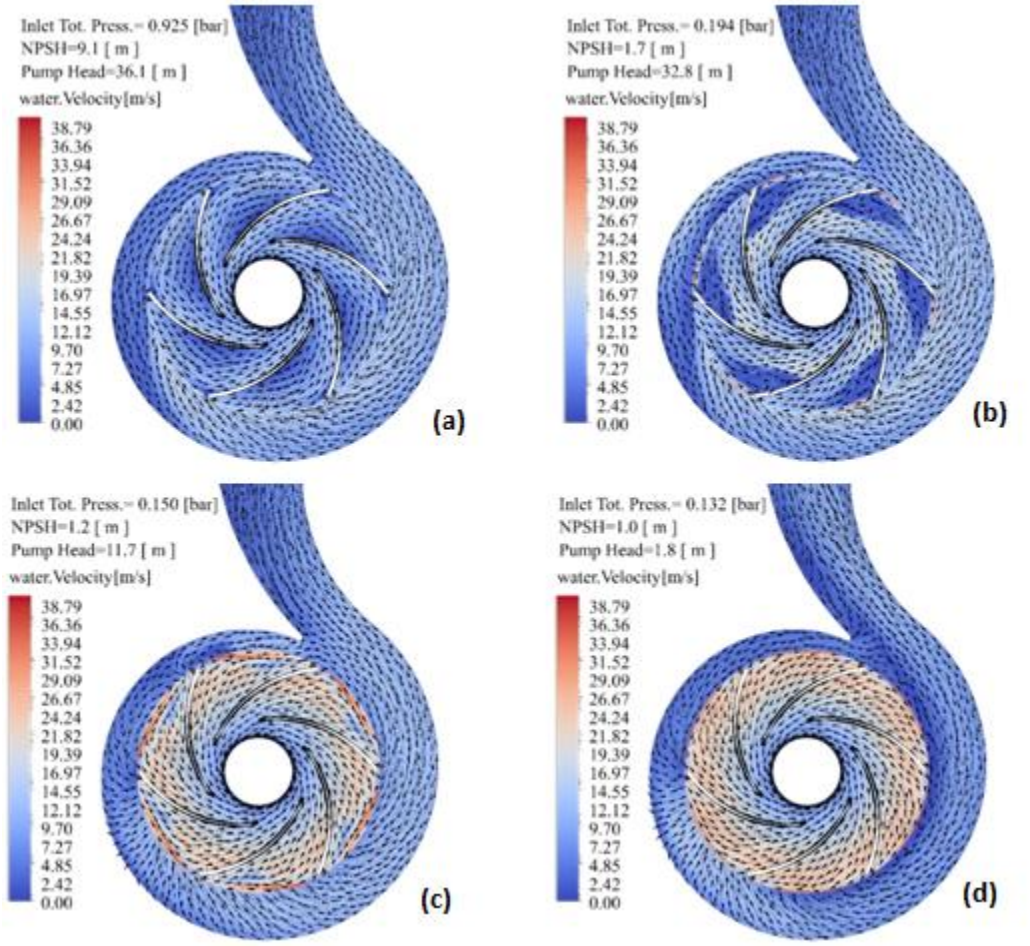

Figure (4): Velocity contours at operating flow rate for inlet total pressure of (a) 0.925 bar, (b) 0.194 bar, (c) 0.15 bar, and (d) 0.132 bar

The time history of the cavitation evolution in between the impeller blades can be casted into three different phases; phase (1) the start of the cavitation, phase (2) cavitation propagates along suction side of the blades while the pump head remains unchanged, and phase (3) cavitation dominates the impeller passage followed by the drop of the pump head, (see Figure (5)). These three phases are discussed further in the coming sections.

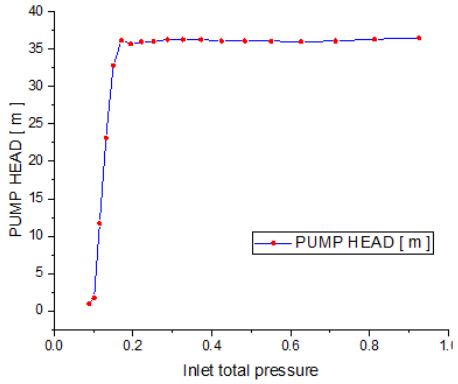

Figure (5): Pump head at variable inlet pressure for design operating conditions

Evolution of Unsteady Cavitation:

The evolution of cavitation and formation of water vapor is illustrated in Figure (6). The cavitation is generated in this study using Rayleigh–Plesset model which is originally derived to be used for solving time-varying bubble radius. However, the Rayleigh–Plesset model is also used for complex cavitating flows as those developed in hydraulic pump cavitating [9]. The Rayleigh–Plesset model was able to reproduce the cavitation physics and track the pump head response accordingly.

The CFD results shown similar trend for the start and evolution of the cavitation. Based on the CFD observation, we recognize three distinct phases during the evolution of the cavitation in a centrifugal pump under transient decrease in inlet pressure. At phase one, the cavitation starts near the leading edge of the impeller blades on the suction side. The most pronounced consequence of the cavitation in this phase is the blade erosion at this region which cause a material loss as the small vapor bubbles collapse near leading edge on the suction side of the pump blades as shown in Figure (7). This is because the leading edge of the blade is the region at which

International Research Journal of Innovations in Engineering and Technology (IRJIET)

ISSN (online): 2581-3048

Volume 6, Issue 6, pp 118-125, June-2022

https://doi.org/10.47001/IRJIET/2022.606015

the flow first engages with impeller and results in high acceleration of the flow which in turn reduces the local static pressure below the saturation point and generate cavitation in that region. This phase occurs at relatively higher inlet pressure and no impact is marked in the pump head. Phase one last for wide range of inlet pressure and is characterized by low or no propagation in the pump cavitation. However, the cavitation in this phase can be considered as inactive since the pump still develops the required head and works at nominal performance.

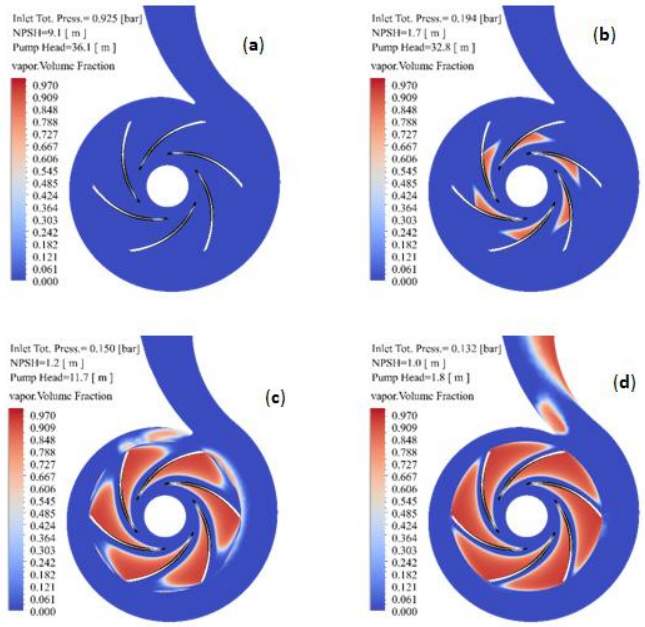

Figure (6): Volume fraction contours at operating flow rate for different inlet pressure of (a) 0.925 bar, (b) 0.194 bar, (c) 0.15 bar, and (d) 0.132 bar

Phase two (2), is started when the cavitation grows and propagate exponentially. This phase take place at inlet pressure of about 0.4 bar. The cavitation in this phase propagates along the suction side from leading to trailing edge of the impeller blade. As it moves downstream, it is getting wider and fills more space in between the blades. The pump head exhibit slight drops during this phase which last for short range of the inlet pressure before it blocks the space between the impeller blade and launches the start of the final phase.

Finally, when the cavitation fills most of the space between impeller blades, the pump head experience dramatic drop which marks the dead point in the pump performance. The pump head drops to zero by the end of this phase and no pressure builds up in the volute domain. This phase occurs at relatively low inlet pressure.

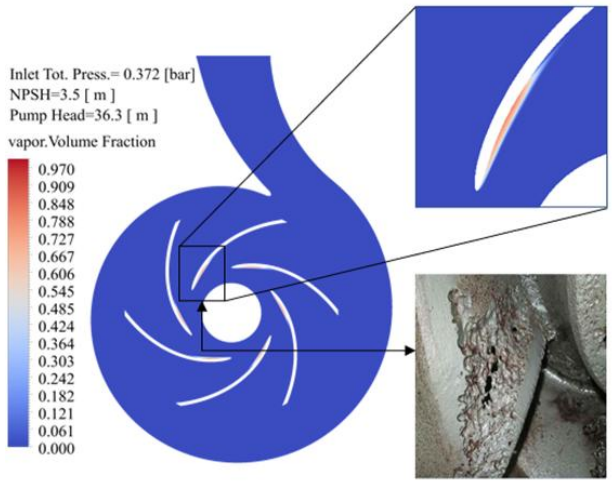

Figure (7): Cavitation erosion

The variation of vapor volume fraction formed by cavitation in the pump impeller domain with the supply pressure is illustrated in Figure (8). It can be observed that cavitation increases exponentially after the inlet pressure drops to 0.3 bar which indicates that the cavitation volume fraction is very sensitive to the inlet pressure during the second phase.

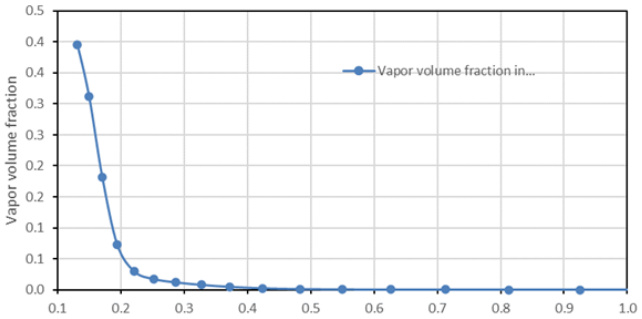

Figure (8): Variation of vapor volume fraction developed in the pump impeller with the inlet pressure at the designed operating conditions

IV. CONCLUSION

Cavitation is a hydrodynamic phenomenon in which the liquid vaporizes in the pump impeller due to local drop in static pressure or when the flow accelerates which in turn decreases the static pressure to a value lower than the saturation pressure. This work involves preliminary one-dimensional centrifugal pump impeller and volute using meanline analysis. The three-dimensional pump impeller is generated by using Bezier polynomial which is used to connect the inlet and outlet main geometrical parameters obtained from the meanline. The meanline analysis flow parameters are used as boundary operating conditions to validate the new design. The operating impeller speed is 2900 rpm, the flow rate is 60 m^3/h, and the design pump head is 39 m. To initiate the cavitation in the designed pump, the inlet

ISSN (online): 2581-3048
Volume 6, Issue 6, pp 118-125, June-2022
https://doi.org/10.47001/IRJIET/2022.606015

total pressure is allowed to decrease with time from atmospheric value to a point where the cavitation is fully developed in the pump impeller and pump head is dropped near zero. This parametric study is set to transient for a purpose of varying the inlet total pressure only and not to involve transient effect on the pump performance. Several conclusions can be taken from this work:

1. The developed pump head and hydraulic efficiency predicted by CFD are lower than the meanline due to the three-dimensional effects such as flow losses including backflow, vortical flow, as well as viscus losses and flow variation in spanwise direction which deviates from meanline design conditions.
2. At normal inlet pressure, the flow is streamed in the impeller passage as well as within the volute and no major vortical flow is observed. This confirms that the meanline is able to predict the blade profile under the design flow conditions. When the inlet pressure decreases to 0.194 bar, flow circulation is, however, developed in the suction side of the impeller blades which can be attributed to the increase of mean flow specific volume due to cavitation.
3. The cavitation resides near leading edge on the suction side causing material loss in this region.
4. The flow is streamed in phase one. Vortical (circulation) flow is developed in phase two. Streamed flow is back during phase three by virtue of displacing more flow due to dramatic increase in the specific volume.
5. Rayleigh-Plesset homogenous cavitation model successfully reproduce the blade suction and pressure sides, pressure recovery in the volute extension, homogenous distribution of the pressure across the interface between moving impeller and fixed volute.

REFERENCES

[1] A. George and M. P, "CFD Analysis Of Performace Charectristics Of Centrifugal Pump Impeller To Minimising Cavitation," *Int. Conf. Curr. Res. Eng. Sci. Technol.*, pp. 24–30, 2016.

[2] W. S. Ocaña, C. Carvajal, J. Poalac\'\in, M. I. Pazmiño, E. S. Jácome, and L. Basantes, "Cavitation Analysis with CFD Techniques of the Impeller of a Centrifugal Pump," *Indian J. Sci. Technol.*, vol. 11, no. 22, pp. 1–6, 2018.

[3] Y. Xu, L. Tan, S. L. Cao, Y. C. Wang, G. Meng, and W. S. Qu, "Influence of blade angle distribution along leading edge on cavitation performance of a centrifugal pump," in *IOP Conference Series: Materials Science and Engineering*, 2015, vol. 72, no. 3, p. 32019.

[4] S. F. Xie, Y. Wang, Z. C. Liu, Z. T. Zhu, C. Ning, and L. F. Zhao, "Optimization of centrifugal pump cavitation performance based on CFD," in *IOP Conference Series: Materials Science and Engineering*, 2015, vol. 72, no. 3, p. 32023.

[5] C. F. X. Ansys, "ANSYS CFX-solver theory guide," *Ansys CFX Release*, vol. 15317, pp. 724–746, 2009.

[6] R. Zgolli, M. Ennouri, and H. Kanfoudi, "Modeling of cavitation in hydraulic turbomachinery," 2016.

[7] F. Bakir, R. Rey, A. Gerber, T. Belamri, and B. Hutchinson, "Numerical and Experimental Investigations of the Cavitating Behavior of an Inducer," *Int. J. Rotating Mach.*, vol. 10, no. 1, pp. 15–25, Jan. 2004, doi: 10.1080/10236210490258034.

[8] X. Li, Z. Zhu, Y. Li, and X. Chen, "Experimental and numerical investigations of head-flow curve instability of a single-stage centrifugal pump with volute casing," *Proc. Inst. Mech. Eng. Part A J. Power Energy*, vol. 230, no. 7, pp. 633–647, Nov. 2016, doi: 10.1177/0957650916663326.

[9] J.-P. Franc, "The Rayleigh-Plesset equation: a simple and powerful tool to understand various aspects of cavitation," in *CISM International Centre for Mechanical Sciences, Courses and Lectures*, vol. 496, Springer, 2007, pp. 1–41.

Citation of this Article:

Hani M. S. Salman, Amir S. Dawood, Younis M. Najim, "Three-Dimensional CFD Simulations of Transient Cavitation in a Centrifugal Pump" Published in *International Research Journal of Innovations in Engineering and Technology - IRJIET*, Volume 6, Issue 6, pp 118-125, June 2022. Article DOI https://doi.org/10.47001/IRJIET/2022.606015

****

